



Missouri University of Science and Technology
Scholars' Mine

Electrical and Computer Engineering Faculty
Research & Creative Works

Electrical and Computer Engineering

01 Jan 2007

Superconducting Magnetic Energy Storage System (SMES) for Improved Dynamic System Performance

Dwaraka S. Padimiti

Badrul H. Chowdhury

Missouri University of Science and Technology, bchow@mst.edu

Follow this and additional works at: https://scholarsmine.mst.edu/ele_comeng_facwork

 Part of the [Electrical and Computer Engineering Commons](#)

Recommended Citation

D. S. Padimiti and B. H. Chowdhury, "Superconducting Magnetic Energy Storage System (SMES) for Improved Dynamic System Performance," *Proceedings of the IEEE Power Engineering Society General Meeting, 2007*, Institute of Electrical and Electronics Engineers (IEEE), Jan 2007.

The definitive version is available at <https://doi.org/10.1109/PES.2007.385739>

This Article - Conference proceedings is brought to you for free and open access by Scholars' Mine. It has been accepted for inclusion in Electrical and Computer Engineering Faculty Research & Creative Works by an authorized administrator of Scholars' Mine. This work is protected by U. S. Copyright Law. Unauthorized use including reproduction for redistribution requires the permission of the copyright holder. For more information, please contact scholarsmine@mst.edu.

Superconducting Magnetic Energy Storage System (SMES) for Improved Dynamic System Performance

Dwaraka S. Padimiti, *Student Member, IEEE*, Badrul H. Chowdhury, *Senior Member, IEEE*

Abstract— A Superconducting Magnetic Energy Storage System (SMES) consists of a high inductance coil emulating a constant current source. Such a SMES system, when connected to a power system, is able to inject/absorb active and reactive power into or from a system. The active power injected into the system is controlled by varying the duty cycle of the switches in the dc-dc chopper while the SMES coil is discharging into the system. The reactive power is controlled by the magnitude of the converter output voltage.

The storage setup is tested on a WSCC 3 machine 9 bus system. The behavior of the system is tested for a three phase fault on the network at different locations. The transient behavior of the system is observed with and without the SMES unit. The SMES unit is able to damp out the post-fault oscillations within a short time.

I. INTRODUCTION

Energy Storage for transmission grid applications has been gaining importance in the last few years. A variety of storage technologies are in the market but the most viable are Compressed Air Energy Storage (CAES) systems, battery energy storage systems (BESS) and Pumped storage Hydroelectric systems and superconducting magnetic energy storage (SMES) [1, 2].

CAES have been used mainly for load leveling purpose. The efficiency of CAES is less than 70%. Some of the disadvantages of Pumped Hydro electric are large unit sizes, topographic and environmental limitations. BESS are presently used in some applications [3]. However, some of its disadvantages include limited life cycle, voltage & current limitations and potential environmental hazards. SMES storage systems can be used to inject both active and reactive power into the grid simultaneously [4, 5]. This can be also be achieved by using BESS, but the efficiency of the SMES system is greater than 98%, which is far better than that of BESS. Also its fast response adds to its performance. The one

This work was supported in part by the Intelligent Systems Center, University of Missouri-Rolla, Rolla, Missouri 65409.

Dwaraka Padimiti is currently a M.S. student in Electrical & Computer Engineering department of the University of Missouri, Rolla, MO 65401 (email dpt46@umr.edu).

Badrul H. Chowdhury is currently a professor in Electrical & Computer Engineering department of the University of Missouri, Rolla, MO 65401 (email: bchow@umr.edu)

major advantage of the SMES coil is that it can discharge large amounts of rated power for a small period of time. Unlimited number of charging and discharging cycles can be carried out.

II. SMES AND BALANCE OF PLANT

A. The SMES Coil

A SMES consists of a high conductance coil which can be treated as a constant current source. Due to its superconducting nature, energy can be stored for a long duration of time without leakage and may then be used to inject active power into the grid whenever there is a disturbance. Niobium-Titanium (NbTi) is the material commonly used to mould the superconductor. The superconductor used here is mainly a 12.5 H inductor with a 100 MJ storage capacity. A SMES coil is wound in a cylindrical shape with a double pancake structure [6]. The SMES coil is designed taking into consideration the self and mutual inductances, turn-turn and turn-ground capacitances that arise due to its construction [7].

A SMES coil can be constructed in many different configurations. One of the most common type is the solenoid type winding. A single solenoid model causes a lot of stray field effects and hence a large number of small size solenoids can be constructed to reduce the stray field but this type of configuration ends up using more conductor material. A modular shaped construction [6, 8] of the toroidal type SMES coil reduces stray field effects to a large extent. The SMES coil used here has a height / width ratio of 3.66 m/1.53 m made of 48 double pancakes. Also, each double pancake has 40 turns.

Fig. 1 shows that the SMES coil is divided into 6 segments. The inductance is in Henry, resistance in ohms and the capacitance is in micro-farad. The resistance accounts for the eddy current losses in the coil and the inductance of 12.5 H has been equally divided among the different segments of the SMES coil. It has been assumed that each segment represents 8 of the double pancakes lumped together. Hence the 48 double pancakes have been reduced to 6 double pancakes where each of the new reduced pancakes itself consists of 8 original double pancakes. This reduction has been done to simplify the mathematical calculations involved.

The capacitance $0.01 \mu F$ accounts for the inter-winding capacitances between the adjacent reduced double pancakes. The winding to ground capacitance is accounted for by the capacitors with a capacitance of $0.0976 \mu F$. The SMES coil is enclosed in a closed container and is grounded by the material that encloses it.

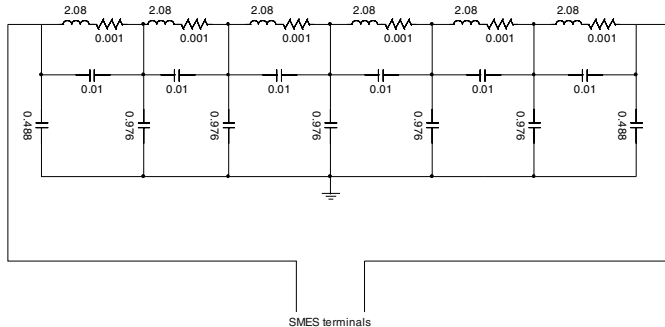


Fig. 1. SMES Coil

B. Power Conditioning System

A power conditioning system (PCS) is required in order to transfer the energy from the SMES coil into the grid. A PCS consists of a dc-dc chopper and a 3 phase voltage source converter (VSC). Using the voltage-angle control strategy, both the active and reactive power can be controlled. A dc-dc chopper is mainly used to keep the current through the SMES coil constant and to transfer the power to the VSC through the dc-link capacitor. The SMES coil along with a dc-dc chopper is connected to the VSC through a dc-link capacitor. This capacitor acts as a temporary dc voltage source for the VSC to inject active/reactive power into the grid.

C. Cryogenic Refrigeration System

The cryogenic system forms the most vital part of the SMES system. Superconducting magnets have to be kept at temperatures in the range of $4 - 10^{\circ}K$ so as to maintain its superconducting nature and carry high currents which create strong magnetic fields [8]. These temperatures can be realized by liquid helium. Hence the liquid helium forms the heart of the cryogenic system. Also, it has to be seen that the SMES coil does not overload since it might lead to the breakdown of the cooling system. If the SMES coil carries a current higher than the rated current, the heat dissipation increases and hence a breach in the cryostat is possible.

III. OPERATION OF SMES

A. Chopper Operation

There are three different modes of operation of the SMES coil. The first mode of operation is the charging of the SMES coil. The SMES coil charges relatively fast to its rated current.

The second mode is the stand-by mode. In this mode the current in the SMES coil effectively circulates in a closed loop, which can also be called as a freewheeling mode. The third mode is the discharge mode, during which the SMES coil discharges into the dc-link capacitor. The three modes are shown in Figs. 2, 3 and 4.

Before discussing the different modes, a GTO (Gate Turnoff Thyristor) in ON state means that the duty cycle of that particular GTO is 1 and a GTO in OFF state means that the duty ratio is 0. All the three modes of operation are explained as follows.

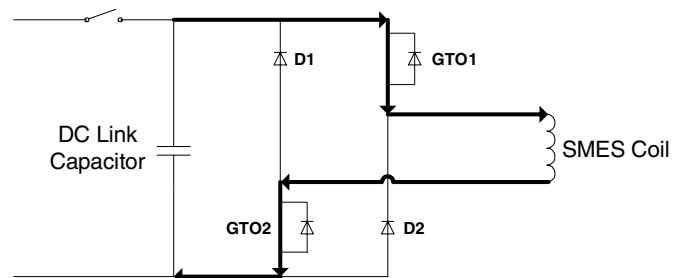


Fig. 2. Charging Mode

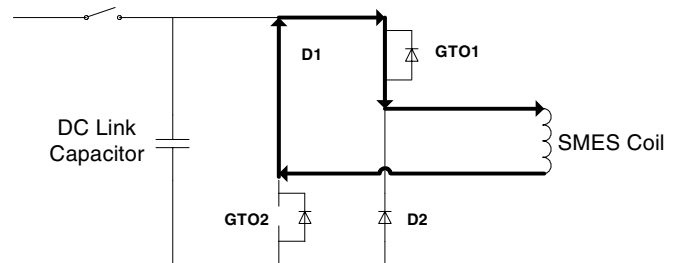


Fig. 3. Freewheeling Mode

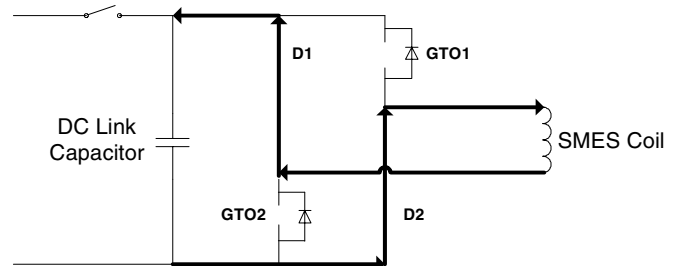


Fig. 4. Discharge Mode

B. SMES Charging Mode

In this mode, the SMES coil is charged to its rated capacity. During charging mode, GTO2 is always in the ON state. GTO1 can be switched ON or OFF in every cycle. The SMES coil charges when the GTO1 is also in the ON state. When the SMES coil is charging, the relationship between the voltage across the SMES coil and the voltage across the dc-link capacitor can be given as

$$V_{SMES} = D * V_{DC} \quad (1)$$

Where V_{SMES} is the voltage across the SMES coil

V_{DC} is the voltage across the dc link capacitor and D is the duty cycle of the GTO1 (defined as the ratio of the GTO ON time to the total time for a complete cycle)

In this particular case, the duty cycle (D) of the GTO1 is kept constant at 1 so that the SMES coil charges at the maximum charging rate possible. In the present simulation, it takes about 3 seconds to charge the coil to its rated current capacity. The current rise through the SMES coil and the

voltage across the SMES coil as captured in the simulation is shown in Fig. 5. It is to be noted that the voltage across the dc link capacitor is 20 KV. All the simulations were carried out using PSCAD.

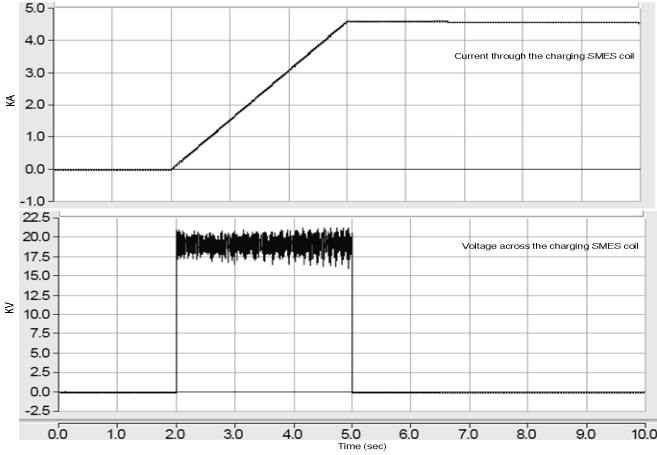


Fig. 5. Current through SMES coil / voltage across SMES coil during charging

C. SMES Freewheeling Mode

The second mode of operation is called the freewheeling mode. In this mode, the current circulates in a closed loop. This is also called the stand by mode. When the SMES coil is in the freewheel mode, one of the two GTO's is OFF. In Fig. 3, it was shown that GTO1 is ON and GTO2 is OFF. During this period, there is no significant amount of loss, as the current through the SMES coil is circulating in a closed loop. Hence, the current remains fairly constant.

D. SMES Discharge Mode

The final mode of operation is the discharge cycle. The current in the SMES coil discharges into the dc link capacitor in this mode of operation. In this mode, the GTO2 is always in the OFF state and the duty cycle of GTO1 can be varied depending on the rate of discharge requirement. During the discharge cycle, to have the maximum rate of discharge, both the GTOs are kept in OFF state. The rate of discharge of the SMES coil can be controlled by making the duty cycle of one of the GTOs to be non-zero. The voltage relationship between the SMES coil and the dc link capacitor during the discharge cycle is given as

$$-V_{SMES} = (1 - D) * V_{DC} \quad (2)$$

In order to have the maximum discharge rate of the SMES coil into the dc link capacitor, the duty cycle of the GTO1 is kept at 0 in the present simulation.

E. Current through the SMES Coil during the Discharge

The current through the SMES coil is shown as the SMES coil discharges at different intervals of time into the 9 bus system, thus providing active power. Also, the voltage across the SMES coil can be noted in Fig. 6. The SMES coil starts discharging into the system at $t = 175$ sec through out the

duration of the fault. After the current in the SMES coil freewheels for about 2 seconds, the active power in the SMES coil is again discharged into the system for a period of 0.25 seconds. The process is again continued for a period of 0.1 second at $t = 178.5$ sec, 0.2 seconds at $t = 179.4$ sec, etc. Such small periods of discharge is continued at each second until $t = 186$ sec.

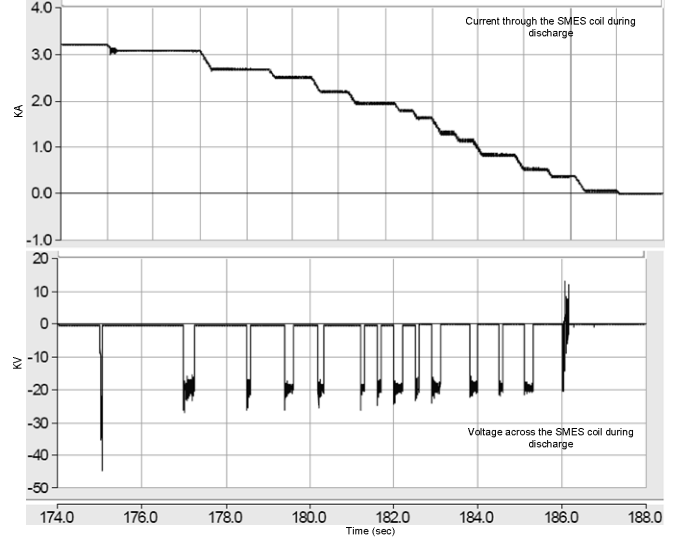


Fig. 6. Current through SMES coil / voltage across SMES coil during discharge

E. Duty Cycle of GTO1 During Discharge

The GTO1 is kept in the OFF position for the duration of the fault in every scenario so that maximum discharge rate of the SMES coil is achieved. However, after the fault is cleared, the rotor angle of the three generators in the system are not at the desired operating point of 377 rad/sec and hence real power is required so as to reach a stable operating point quickly. Hence the SMES coil is discharged into the dc link capacitor even after the fault is cleared. The discharge is done at different time periods for small intervals of time. The duty cycle for the same can be seen in Fig. 7.

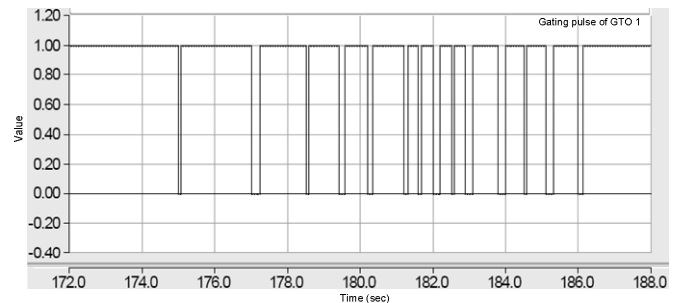


Fig. 7. Gating pulse of GTO1

IV. 3 MACHINE 9 BUS WSCC SYSTEM

The 9 bus system used for the simulation is shown in Fig. 8. Table 1 shows the line parameters of the 9 bus system. The power flow data is given in the Appendix.

The generator at bus 1 is taken as the swing bus with a voltage of 1.04 p.u. The generators at buses 2 and 3 are taken to be PV buses with scheduled voltage at 1.025 p.u.

TABLE I
LINE PARAMETERS OF THE 9 BUS SYSTEM

Line	Resistance (p.u)	Reactance (p.u)	Admittance (p.u)
1-4	0.0000	0.0576	j0.0000
4-5	0.0170	0.0920	j0.0790
5-6	0.0390	0.1700	j0.1790
6-3	0.0000	0.0586	j0.0000
6-7	0.0119	0.1008	j0.1045
7-8	0.0085	0.0720	j0.7450
8-2	0.0000	0.0625	j0.0000
8-9	0.0320	0.1610	j0.1530
9-4	0.0100	0.0850	j0.0880

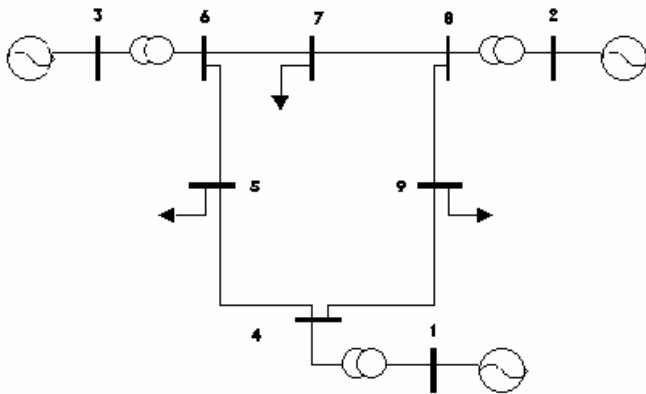


Fig. 8. WSCC 9 bus system

V. RESULTS

The simulations are done on a WSCC 3 machine 9 bus system. The SMES system was initially placed between buses 4 and 9 (nearer to bus 4) and later, the faults were simulated with the SMES system placed at Bus 7. A three phase ground fault was created at $t = 175$ sec for a period of 70 ms (milliseconds) at different locations in the 9 bus system and the overall performance of the system is compared with and without the SMES system. The angular frequency of the three generators is compared in both the scenarios. The duration of the simulation is restricted to 350 seconds.

A. Simulations With the SMES at Bus 4

Fault Simulated Between Buses 4 and 9. During the simulation, from time $t = 5$ sec to $t = 40$ sec, oscillations occur in the system due to the startup of the system from cold conditions. These oscillations can be seen in Fig. 9 and subsequent figures where rotor angles have been compared. In this simulation, the three phase fault is created between buses

4 and 9 (nearer to bus 4). The voltage across the dc link capacitor, the active and reactive power consumed by the SMES system during the charging of the SMES coil is shown in Figs. 9 (a), (b) and (c), respectively.

While simulating, the active power injected into the 9 bus system is taken as the positive convention. It can be seen in Fig. 9 that the active power is negative as it is charging from $t = 2$ sec till $t = 5$ sec. Hence the active power is being absorbed by the SMES system. The change in the reactive power and the dc-link capacitor voltage at $t = 5$ sec is due to the change in the operation of the SMES coil from charging mode to freewheeling mode. The comparison of the rotor angles of the three generators is shown in Fig. 10. It can be clearly seen that the performance of the system improves when the SMES system discharges active power into the system as compared to the system with the SMES.

Fault Simulated Between Buses 8 and 7

The performance of the 9 bus system improves very much as compared to the previous fault locations. The system frequency is restored in less than four seconds after the fault. As the fault was simulated at a location distant from the point of connection of the SMES system, its performance during and after the fault was completely realizable. The system restores stability in a remarkably less time which makes bus 4 the ideal location for the placement of the SMES system for a fault away from it such as between buses 7 and 8. The results are shown in Fig. 11. The voltage across the dc link capacitor, active and reactive power from the SMES system during the overall simulation are shown in Fig. 12.

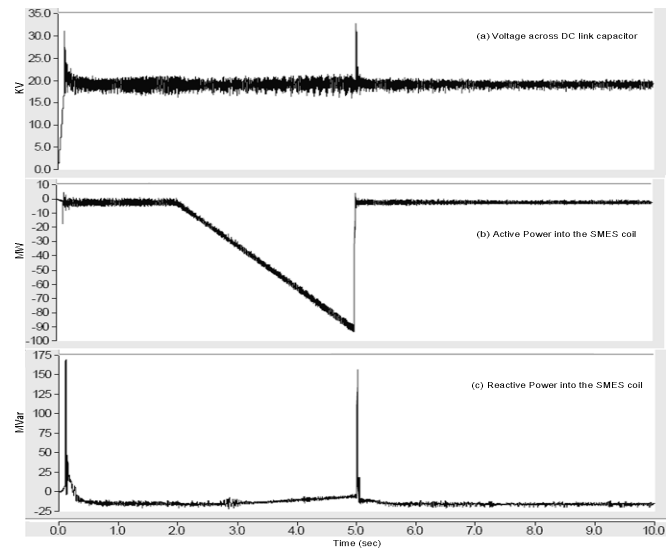


Fig. 9. Active and reactive power into the SMES during charging cycle

B. Simulations with the SMES at Bus 7

Fault Simulated Between Buses 8 and 9

The SMES coil is charged from $t = 2$ sec until $t = 5$ sec and is made to freewheel till $t = 175$ sec at which point, a three phase-ground fault is simulated between buses 8 and 9 (closer to bus 8). The variations in the rotor speed of the three

generators with and without the SMES system were compared and are shown in Fig. 13.

It can be clearly seen from Fig. 12 that the rotor speed is under control when the SMES system discharges into the system as against the system without the SMES system. This is due to the supply of both active and reactive power by the SMES into the system during and after the fault. The dc-link capacitor voltage, active and reactive power injected into the system during the fault can be seen in Fig. 14 and for the complete simulation can be seen in Fig. 15.

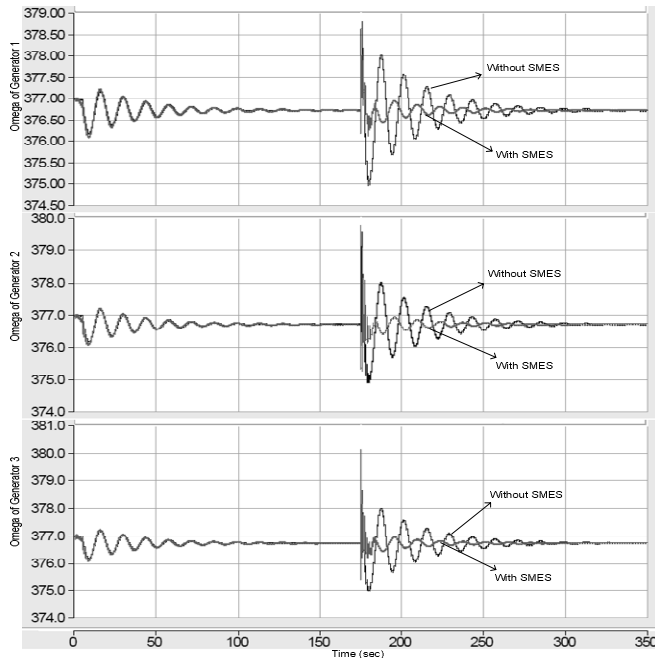


Fig. 10. Comparison of rotor speed for a three phase fault between bus 4 & 9

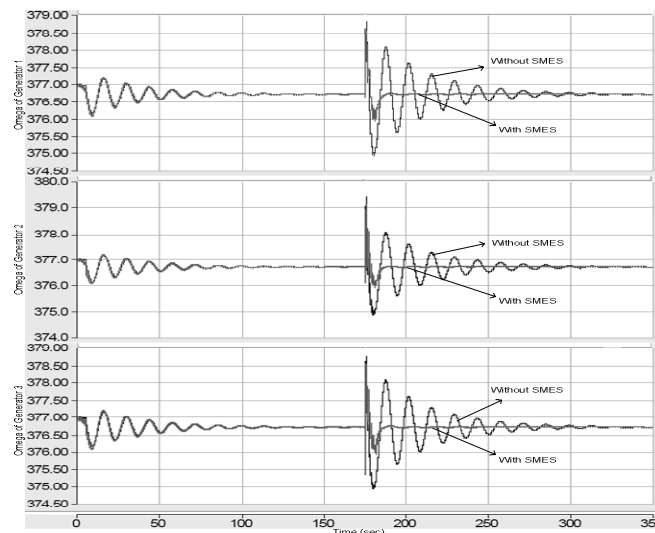


Fig. 11. Comparison of rotor speed for a three phase fault between buses 8 & 7

From Fig. 14, it can be seen that an average active power of about 70 MW is being discharged into the system during the fault at $t = 175$ sec. Also, there is a significant amount of reactive power being injected into the system.

VI. CONCLUSION

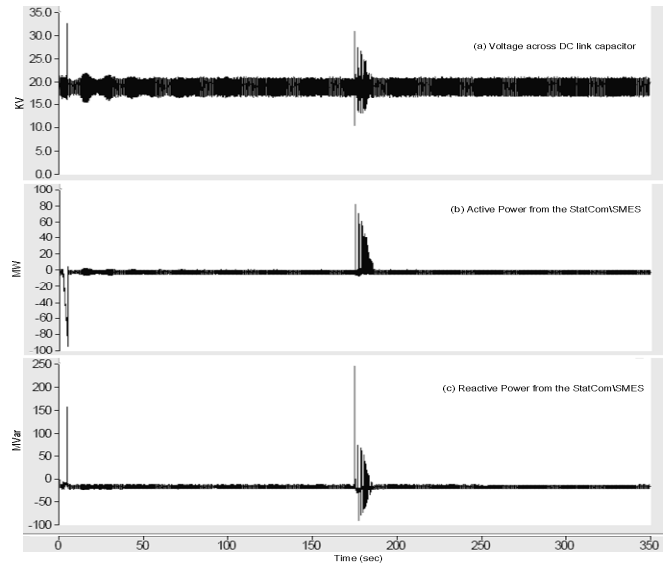


Fig. 12. Active and reactive power into the SMES system

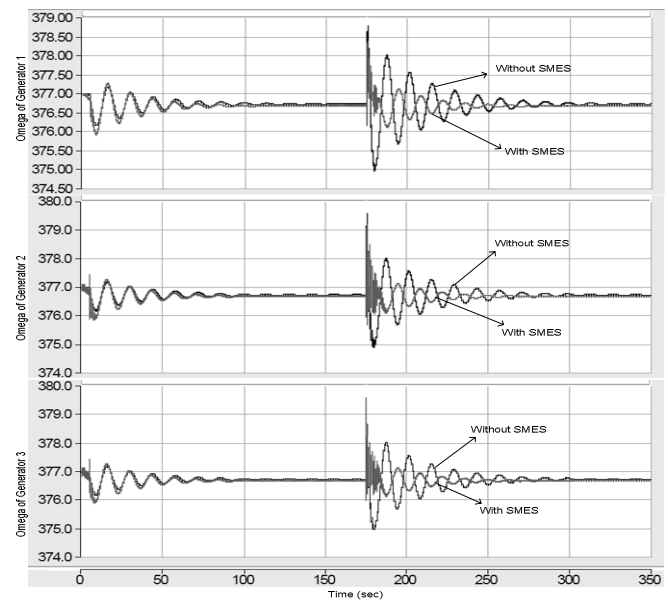


Fig. 13. Comparison of rotor speed for a three phase fault between buses 8 & 9

The use of SMES can be seen as a power quality device as well as for damping of power system oscillations. Such a SMES system was integrated on a simple 3 machine 9 bus power system and its performance was evaluated for 3 phase faults at various location. The main advantage of the SMES system compared to other energy storage technologies/devices is its ability to inject active and reactive power into the power system simultaneously. The system is capable of discharging large amounts of energy for short periods of time thus helping with dynamic performance.

With the advancement in the science of superconductor technology, the cost of installation of the SMES systems is eventually going to be comparable to that of the existing storage technologies.

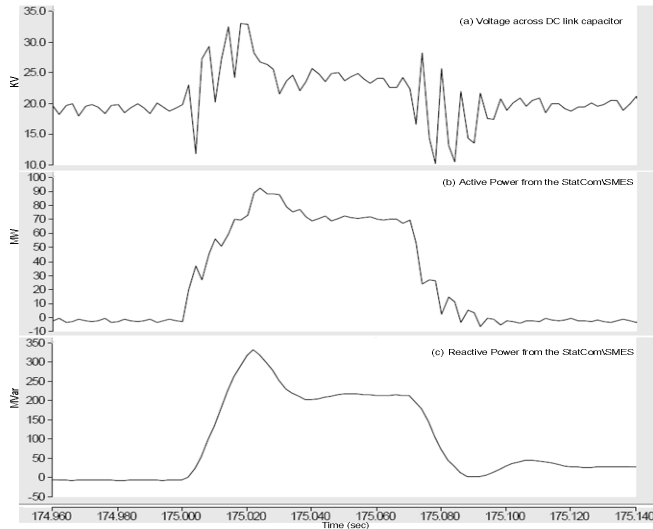


Fig. 14 Active and reactive power injected into the system by the SMES

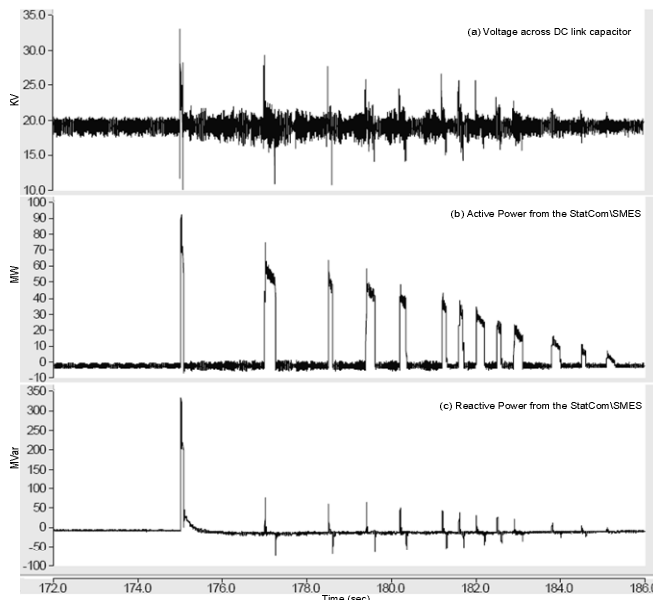


Fig. 15. Active and reactive power flows of the SMES during the simulation

VII. REFERENCES

- [1] C. A. Luongo, "Superconducting storage systems: An overview," *IEEE Transactions on Magnetics*, Vol. 32, Issue 4, Part 1, pp. 2214 – 2223, Jul 1996W.-K. Chen, *Linear Networks and Systems* (Book style). Belmont, CA: Wadsworth, 1993, pp. 123–135.
- [2] W. V. Torre and S. Eckroad, "Improving power delivery through the application of superconducting magnetic energy storage (SMES)," *IEEE Power Engineering Society Winter Meeting*, Vol. 1, pp. 81 – 87, 28 Jan – 1 Feb, 2001.
- [3] P. F. Ribeiro, B. K. Johnson, M. L. Crow, A. Arsoy and Y. Liu, "Energy storage systems for advanced power applications," *Proceedings of the IEEE*, Vol. 89, Issue 12, pp. 1744 – 1756, Dec. 2001.
- [4] C. J. Wu and Y. S. Lee, "Application of simultaneous active and reactive power modulation of superconducting magnetic energy storage unit to

damp turbine-generator sub synchronous oscillations," *IEEE Transactions on Energy Conversion*, Vol. 8, Issue 1, pp. 63 – 70, Mar 1993.

- [5] J. J. Skiles, R. L. Kustom, K. P. Ko, V. Wong, K. S. Ko, F. Vong and K. Klontz, "Performance of a power conversion system for superconducting magnetic energy storage (SMES)," *IEEE Transactions on Power Systems*, Vol. 11, Issue 4, pp. 1718 – 1723, Nov, 1996.
- [6] J. H. Kim, W. S. Kim, S. Y. Hahn, J. M. Lee, M. H. Rue, B. H. Cho, C. I. Hwan, H. and K. Jung, "Characteristic test of HTS pancake coil modules for small-sized SMES," *IEEE Transactions on Applied Superconductivity*; Vol. 15, Issue 2, Part 2, pp: 1919–1922, June 2005.
- [7] A. B. Arsoy, Z. Wang, Y. Liu and P. F. Ribeiro, "Transient modeling and simulation of a SMES coil and the power electronics interface," *IEEE Transactions on Applied Superconductivity*, Vol. 9, Issue 4, pp. 4715 – 4724, Dec. 1999.
- [8] Ise, T and Murakami, Y, "Modular based design for a small to medium scale toroidal type SMES," *IEEE Transactions on Applied Superconductivity*, Vol. 4, Issue 2, pp. 51-55, June 1994.
- [9] A. Bautista, P. Esteban, L. Gracia-Tabares, C. Peon, E. Martinez, J. Sese, A. Camon, C. Rillo and R. Iturbe, "Design, manufacturing and cold test of a superconducting coil and its cryostat for SMES applications," *IEEE Transactions on Applied Superconductivity*, Vol. 9, Issue 2, Part 1, pp. 853 – 856, June 1997.

VIII. APPENDIX

POWER FLOW DATA

Bus No.	Type	Voltage (PU)	Pg (PU)	Qg (PU)	-PI	-QI
1	(swing)	1.04∠0°	0.716	0.27	-	-
2	(P-V)	1.025∠9.3°	1.63	0.067	-	-
3	(P-V)	1.025∠4.7°	0.85	-0.109	-	-
4	(P-Q)	-	-	-	-	-
5	(P-Q)	-	-	-	0.9	0.3
6	(P-Q)	-	-	-	-	-
7	(P-Q)	-	-	-	1.0	0.35
8	(P-Q)	-	-	-	-	-
9	(P-Q)	-	-	-	1.25	0.50

IX. BIOGRAPHIES

Dwaraka Padimithi obtained his Bachelor's degree in Electrical and Electronics Engineering from Osmania University in May 2004. He is pursuing his M.S. Degree in Electrical Engineering from the University of Missouri – Rolla. His research interests include power system stability and power quality.

Badrul H. Chowdhury (M'1983, SM'1993) obtained his Ph.D. degree in Electrical Engineering from Virginia Tech, Blacksburg, VA in 1987. He is currently a Professor in the Electrical & Computer Engineering department of the University of Missouri-Rolla. From 1987 to 1998 he was with the University of Wyoming's Electrical Engineering department. Dr. Chowdhury's research interests are in power system modeling, analysis and control and distributed generation. He teaches courses in power systems, power quality and power electronics.